Chapter 2

Quality-Yield Measure for Very Low Fraction Defective

In this chapter, we first rewrite the quality yield as representation of process yield and expected relative loss, focusing on production processes with very low fraction of defectives. We then obtain a lower confidence bound on process capability index C_{pk} and an upper confidence bound on the expected relative loss to convert the estimated quality yield value into a reliable lower confidence bound. The chapter is organized as follows. Section 2.1 presents the comparisons of yield and Q-yield, with some illustrative examples. Section 2.2 investigates the estimator of quality yield. Since $Y - L_e$ provides a lower bound on the quality yield, estimations of process yield Y and process loss L_e are also explored. In Section 2.3, we propose a reliable method to obtain a lower confidence bound on quality yield. Section 2.4 presents an application example of the amplified pressure sensor (APS). Section 2.5 demonstrates the proposed methodology by calculating the quality yield for pressure sensor product.

2.1 Comparisons of Yield and Quality Yield

Process yield is currently defined as the percentage of the processed product units passing the inspections. Units are inspected according to specification limits placed on various key product characteristics and sorted into two categories: passed (conforming) and rejected (defectives). Use of yield as a quality measure implies that each rejected unit costs the factory an additional amount (scrap or repair) while each passed unit costs the factory nothing additional. By inference, all passed units are equally acceptable to the next-in-line customer. Customer in this sense refers to any user of goods such as materials, components, subassemblies, assemblies, or systems.

However, customers do notice unit-to-unit difference in these characteristics, especially when the variance is large and/or the mean is offset from the target. A more customer-oriented measure Y_q is then proposed to account for both the fraction of defectives and variation from target for the passed units. Penalty to the yield increases as the departure from the target value T increases. When all conforming products are on target, then $Y_q = Y$. Figures 1(a)-1(b) display two normally distributed processes, $N(\mu = T, \sigma = d/3)$, and $N(\mu = T + d/3, \sigma = d/6)$, respectively, with the quadratic loss function. The latter process has a higher yield but with a lower Q-yield since it has larger departure from the target value than the former. Furthermore, if the process characteristic X follows uniform distribution, $U(LSL, USL)$, then the yield is $Y = 1.00$(100% conforming) and Q-yield is $Y_q = 0.665$ (66.5% perfect), respectively. Obviously, this is a low-quality process. On the other hand, if X follows the chi-square distribution with degrees of freedom three, the yield would be $Y = 0.888$ (88.8% conforming) and Q-yield would be $Y_q = 0.62$ (62% perfect) (see Figures 1(c)-1(d)).

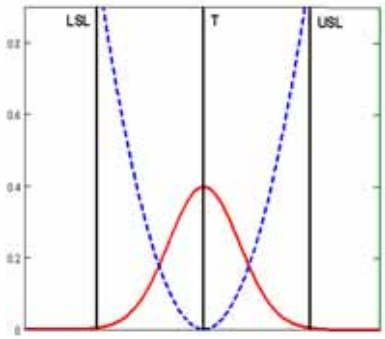

Figure 1(a). Plots of process $N(T, d/3)$ with loss function.

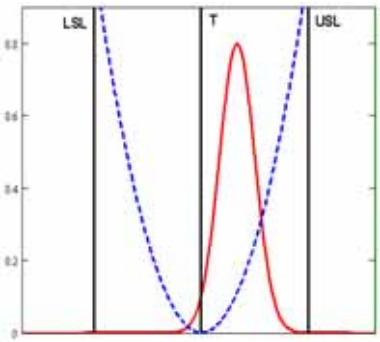

Figure 1(b). Plots of process $N(T + d/3, d/6)$ with loss function.

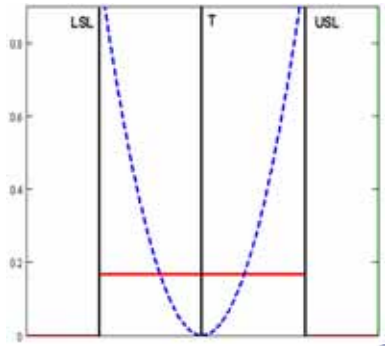

Figure 1(c). Plots of process $U(LSL,USL)$ with loss function.

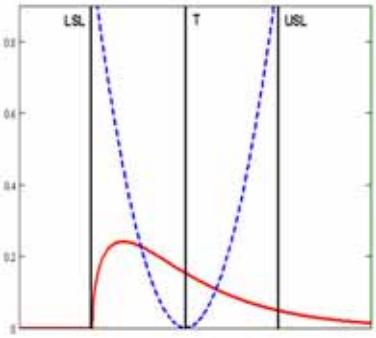

Figure 1(d). Plots of process $\chi^2(3)$ with loss function.

To extend the applicability of the plot for normally distributed processes, we rewrite the definition of Y and Y_q as a function of $C_d = (\mu - T)/d$ and $C_v = \sigma / d$. Noting that the sub-index C_d measures the departure ratio, and the sub-index C_v measures the process variation relative to the specification tolerances. The value of C_d (abscissa) we considered goes from –2 to 2 and hence μ goes from $T - 2d$ to $T + 2d$. Moreover, the value of C_v (ordinate) goes from 0 to 1 to cover a wide range of σ. Therefore, using C_d as the *x*-axis, C_v as the *y*-axis, we can plot the surface of Y and Y_q with various $-2 \le C_d \le 2$ and $0 \le C_v \le 1$, which displayed in Figures 2(a)-(b), respectively. Figures 2(c)-(d) display the cross-section plot of Y and Y_q versus $-2 \le C_d \le 2$ for various C_v =1/6, 1/4, 1/3, 1/2, 1 (top to bottom in plot). We note that the plots of Y and Y_q are invariable irrespective of the value of the specification limits. Processes with multiple characteristics having different characteristic specification limits can thus be plotted simultaneously on a single chart.

Therefore, high Q-yield values are desirable and can be viewed as improved product quality from the customer's viewpoint. Q-yield is more flexible because it compares the quality of different characteristics of a product on a single percentage scale, and indicates how close a product comes to meeting 100% customer satisfaction. Comparing with the existing capability indices, we note that those capability indices rely on the underlying assumption of normal distribution. Although new capability indices have been developed for non-normal distributions (for example, Clements (1989) and Johnson-Kotz-

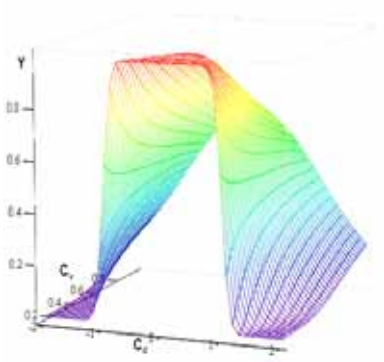

Figure 2(a). Surface plot of Y versus $-2 \le C_d \le 2$ and $0 \le C_v \le 1$.

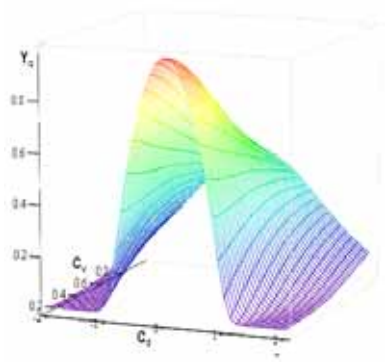

Figure 2(b). Surface plot of Y_q versus $-2 \le C_d \le 2$ and $0 \le C_v \le 1$.

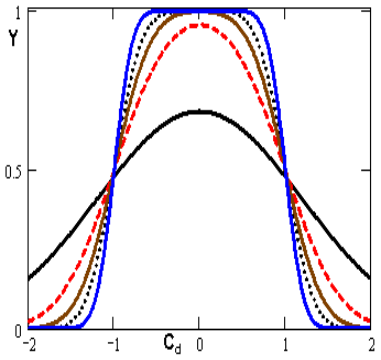

Figure 2(c). Plots of Y versus $-2 \le C_d \le 2$ for various C_v =1/6, 1/4, 1/3, 1/2, 1 (top to bottom).

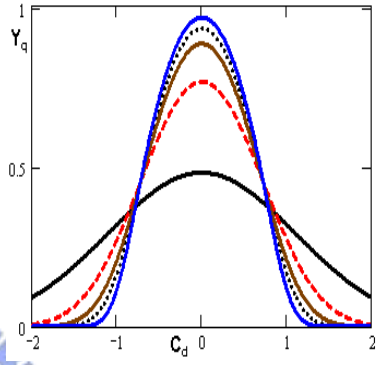

Figure 2(d). Plots of Y_q versus $-2 \le C_d \le 2$ for various C_v =1/6, 1/4, 1/3, 1/2, 1 (top to bottom).

Pearn (1994) methods). Those indices are more complicated to analyze and harder to interpret, and are sensitive to data peculiarities such as bimodality or truncation. Second, these indices do not explicitly account for the manufacturing cost or customer's loss. Capability indices are generally defined with respect to the specification limits rather than the customer's functional limits. Table 1 summarizes values of those indices for some cases to illustrate the differences among Y, Y_q and C_p, C_{pk}, C_{pm}, C_{pmk}.

Table 1. Comparisons of yield, Q-yield, and C_p, C_{pk}, C_{pm}, C_{pmk}.

Case	Y %	Y_q %	C_p	C_{pk}	C_{pm}	C_{pmk}
$N(T, d)$	68.27	48.39	0.33	0.33	0.33	0.33
$N(T, d/2)$	95.45	76.99	0.67	0.67	0.67	0.67
$N(T, d/3)$	99.73	88.94	1.00	1.00	1.00	1.00
$N(T, d/4)$	99.99	93.75	1.33	1.33	1.33	1.33
$N(T \pm d/3, d/2)$	90.50	69.13	0.67	0.44	0.55	0.37
$N(T \pm d/3, d/3)$	97.72	78.41	1.00	0.67	0.71	0.47
$N(T \pm d/3, d/4)$	99.62	82.70	1.33	0.89	0.80	0.53
$N(T \pm d/3, d/6)$	99.997	86.11	2.00	1.33	0.89	0.60

2.2 Estimation of Quality Yield

Ng and Tsui (1992) proposed a sample estimator based on a finite population of products. Suppose $X_1, X_2, ..., X_n$ denote the sample measurements of product characteristics. It follows that yield and Q-yield are estimated by collected sample data can be defines as,

$$\hat{Y} = \sum_{LSL \le X_i \le USL} \frac{1}{n}, \tag{2.1}$$

$$\hat{Y_q} = \sum_{LSL \le X_i \le USL} \left[\frac{1 - (X_i - T)^2 / d^2}{n} \right]. \tag{2.2}$$

The sampling distribution and sampling errors are investigated. The decision maker would be interested in a lower bound on the quality yield rather than just the sample point estimate. Further, as the rapid advancement of manufacturing technology and customers demand, when the fraction of defectives is very low, such as in parts per million (ppm), products almost all fall between LSL and USL, one cannot even observe a defective item on inspection for a reasonable sample size. Thus, such approach is not applicable for the low defective processes (since the sample point estimate is almost certain be zero). The quality yield index Y_q can be rewritten as the following:

$$Y_q = Y - \int_{LSL}^{USL} \left[\frac{(x - T)^2}{d^2} \right] dF(x) \ge Y - L_e. \tag{2.3}$$

Thus, the measure $Y - L_e$ provides a lower bound on the quality yield Y_q. For processes with very low fraction of defectives, the approximation of Y_q using $Y - L_e$ would be quite accurate. Subsequently, we discuss the estimators of process yield Y and process loss L_e.

Estimation of Process Yield Y

The index C_{pk} is yield-based which provides a lower bound on the process yield; that is, $2\Phi(3C_{pk}) - 1 \le \text{yield} \le \Phi(3C_{pk})$ (see Boyles (1991)). Table 2 displays some index values with two-sided specifications and the corresponding maximal non-conforming units in parts per million (ppm) calculated by the formula $2 \times 10^6 \times [1 - \Phi(3C_{pk})]$, for a normally distributed process.

Table 2. Some C_{pk} index values with the corresponding defective units (in ppm) for a normally distributed process.

C_{pk}	0.7	0.8	0.9	1	1.1	1.2	1.3	1.33
ppm	35729	16395	6934	2700	967	318	96	66
C_{pk}	1.4	1.5	1.6	1.67	1.7	1.8	1.9	2.0
ppm	27	6.795	1.587	0.544	0.34	0.067	0.012	0.002

When $C_{pk} = C$, $b = d/\sigma$ can be expressed as $b = 3C + |\xi|$. Thus, the index C_{pk} may be expressed as a function of the characteristic parameter ξ,

$$C_{pk} = \frac{d - |\mu - M|}{3\sigma} = \frac{d/\sigma - |\xi|}{3}, \text{ where } \xi = (\mu - M)/\sigma. \qquad (2.4)$$

Construction of the exact lower confidence bounds on C_{pk} is complicated since the distribution of $\hat{C}_{pk}$ involves the joint distribution of two non-central *t*-distributed random variables, or alternatively, the joint distribution of the folded-normal and the chi-square random variables, with an unknown process parameter even when the samples are given (Pearn *et al.* (1992)). Numerous methods for obtaining approximate confidence bounds of C_{pk} have been proposed, including Bissell (1990), Chou *et al.* (1990), Zhang *et al.* (1990), Porter and Oakland (1991), Kushler and Hurley (1992), Rodridguez (1992), Nagata and Nagahata (1994), Tang *et al.* (1997) and many others.

Using the integration technique similar to that presented in Vännman (1997), Pearn and Lin (2002) obtained an exactly explicit form of the cumulative distribution function of the natural estimator $\hat{C}_{pk} = (d - |\bar{X} - M|)/(3S_{n-1})$, where $S_{n-1} = [\sum_{i=1}^{n}(X_i - \bar{X})^2/(n-1)]^{1/2}$, under the normal assumption, which is expressed in terms of a mixture of the chi-square distribution and the normal distribution, for $x > 0$, where $G(\cdot)$ is the cumulative distribution function of the chi-square distribution with degree of freedom $n-1$, χ^2_{n-1}, and $\phi(\cdot)$ is the probability density function of the standard normal distribution,

$$F_{\hat{C}_{pk}}(x) = 1 - \int_0^{b\sqrt{n}} G\left(\frac{(n-1)(b\sqrt{n} - t)^2}{9nx^2}\right)\left[\phi(t + \xi\sqrt{n}) + \phi(t - \xi\sqrt{n})\right]dt. \qquad (2.5)$$

(A brief derivation of the cumulative distribution function of $\hat{C}_{pk}$ is included in the Appendix A.) Hence, given the sample of size *n*, the confidence level γ, the estimated value $\hat{C}_{pk}$, and the parameter ξ, using numerical integration technique with iterations, the $100\gamma\%$ lower confidence bounds for C_{pk}, C_L, where $b_L = 3C_L + |\xi|$, can be obtained by solving the following equation,

$$\int_0^{b_L\sqrt{n}} G\left(\frac{(n-1)(b_L\sqrt{n} - t)^2}{9n\hat{C}_{pk}^2}\right)\left[\phi(t + \xi\sqrt{n}) + \phi(t - \xi\sqrt{n})\right]dt = 1 - \gamma. \qquad (2.6)$$

An $100\gamma\%$ lower confidence bound on the process yield *Y* can then be expressed as $2\Phi(3C_L) - 1$.

However, since the process parameters μ and σ are unknown, then the distribution characteristic parameter, ξ is also unknown, which has to be estimated in real applications, naturally done by substituting μ and σ with the sample mean $\bar{X}$ and the sample standard deviation *S*. Such approach (and most existing methods) introduces additional sampling errors from estimating ξ in finding the lower confidence bounds, which certainly would make our decisions less reliable and provide less quality assurance to the customers. To

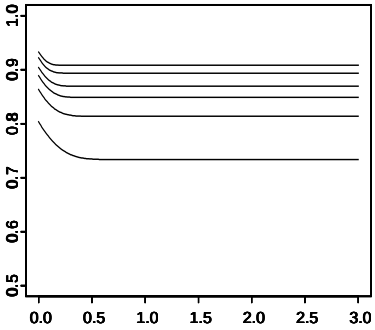

Figure 3(a). Plots of C_L vs $|\xi|$ for $\hat{C}_{pk}$ = 1.00, n = 25, 50, 75, 100, 150, 200 (bottom to top).

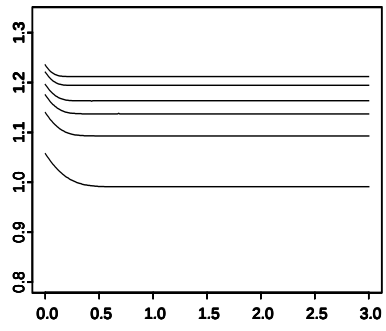

Figure 3(b). Plots of C_L vs $|\xi|$ for $\hat{C}_{pk}$ = 1.33, n = 25, 50, 75, 100, 150, 200 (bottom to top).

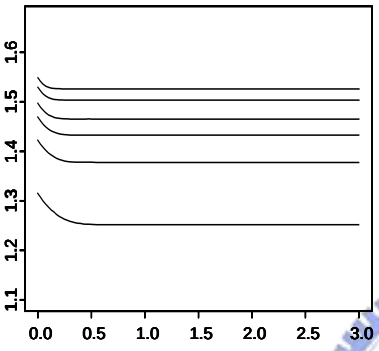

Figure 3(c). Plots of C_L vs $|\xi|$ for $\hat{C}_{pk}$ = 1.67, n = 25, 50, 75, 100, 150, 200 (bottom to top).

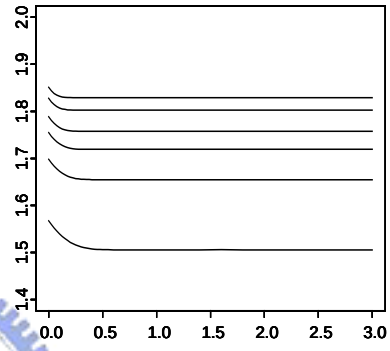

Figure 3(d). Plots of C_L vs $|\xi|$ for $\hat{C}_{pk}$ = 2.00, n = 25, 50, 75, 100, 150, 200 (bottom to top).

eliminate the need for further estimating the distribution characteristic parameter ξ, we examine the behavior of the lower confidence bound values C_L against the parameter ξ. The results indicate that the lower confidence bound is decreasing in ξ and reaches its minimum at $\xi = 1.00$ in all cases, and stays at the same value for $\xi \geq 1.00$ with accuracy up to 10^{-4}. Figures 3(a)-3(d) plot the curves of the lower confidence bound, C_L, versus the parameter ξ = 0(0.05)3.00, n = 25, 50, 75, 100, 150, 200 with confidence level γ = 0.95, for $\hat{C}_{pk}$ = 1.00, 1.33, 1.67 and 2.00, respectively. Hence, for practical purpose we may solve above equation with $\hat{\xi} = \xi = 1.00$ to calculate the required lower confidence bounds for given $\hat{C}_{pk}$, n, and γ, without having to further estimate the parameter ξ. Thus, based on such approach, the γ confidence level can be ensured and the decisions made are indeed more reliable.

Estimation of Process Loss L_e

Johnson (1992) proposed the relative expected squared error loss L_e by approaching capability from the point of view of the loss function. However, here the opposite concept of worth was used. It was assumed that a characteristic achieves its maximum worth W_T, when $X = T$, with decreasing values of worth as X moves away from the target value T (eventually the worth becomes zero, then negative). The worth function can be described by $W_T - k(X - T)^2$, for $W_T \geq k(X - T)^2$, and it will become zero when $|X - T| = (W_T / k)^{1/2}$.

Johnson (1992) viewed the pair $(T+(W_T/k)^{1/2}, T-(W_T/k)^{1/2})$ in the role of specification limits for C_{pm} and defined $d=(W_T/k)^{1/2}$ by assuming the product has zero worth outside the specifications. The ratio of worth to maximum worth is called the relative worth and can be defined as

$$W(X)=1-\frac{k(X-T)^2}{W_T}=1-\frac{(X-T)^2}{d^2}, \tag{2.7}$$

where $(X-T)^2/d^2$ is the relative loss. The expected relative loss, $L_e=E[(X-T)^2]/d^2$, is used to quantify capability, and is effectively equivalent to C_{pm}, since

$$L_e=(3C_{pm})^{-2}. \tag{2.8}$$

A natural unbiased estimator of L_e is

$$\hat{L}_e=\frac{1}{nd^2}\sum_{i=1}^{n}(X_i-T)^2. \tag{2.9}$$

2.3 Lower Confidence Bounds on Quality Yield

Now we deal with the lower confidence limit on the quality yield. Given a sample of size *n*, the confidence level γ, the estimated value $\hat{C}_{pk}$, and the estimated relative loss $\hat{L}_e$, the lower confidence bounds of Y_q can be easily obtained by some mathematical manipulations. The $100\gamma\%$ lower confidence bound of Y_q can be expressed as:

$$P(Y_q \ge L_{Y_q}) \ge P(Y \ge L_Y, Y_q \ge L_{Y_q}) \ge \gamma \quad \text{and}$$

$$L_{Y_q}=L_Y-U_{L_e}=2\Phi(3C_L)-1-\left[\frac{n+\hat{\lambda}}{\chi'^2_n(1-\gamma_2;\hat{\lambda})}\right]\hat{L}_e, \tag{2.10}$$

where L_Y is a lower $100\gamma_1\%$ confidence bound on Y, U_{L_e} is an upper $100\gamma_2\%$ confidence bound on L_e, and $\gamma=\gamma_1\times\gamma_2$. All derivations are shown below. A lower $100\gamma\%$ confidence bound for Y_q and Y simultaneously can be derived as (for processes with very low fraction defective, we use approximate Y_q by $Y-L_e$ in the following derivation):

$$\begin{aligned}
P(Y \ge L_Y, Y_q \ge L_{Y_q}) &= P(Y \ge L_Y)\times P(Y_q \ge L_{Yq} \mid Y \ge L_Y) \\
&= P(Y \ge L_Y)\times P(L_e \le Y-L_{Y_q} \mid Y \ge L_Y) \\
&\ge P(Y \ge L_Y)\times P(L_e \le L_Y-L_{Y_q}) \\
&= \gamma_1\times\gamma_2=\gamma.
\end{aligned} \tag{2.11}$$

As pointed out earlier, the yield-based index C_{pk} gives a lower bound on the process yield. Hence, the probability $P(Y \ge L_Y)$ is equivalent to the probability $P(C_{pk} \ge C_L)$. Solve $P(Y \ge L_Y)=\gamma_1$ for L_Y, we obtain $L_Y=2\Phi(3C_L)-1$, where C_L is the $100\gamma_1\%$ lower confidence bound on C_{pk}. Next, we

proceed with the expression $P(L_e \le L_Y - L_{Y_q}) = \gamma_2$. Under normality assumption, $(n+\lambda)\hat{L}_e / L_e$ is distributed as $\chi_n'^2(\lambda)$, a non-central chi-squared distribution with n degrees of freedom and non-centrality parameter $\lambda = n(\mu - T)^2 / \sigma^2$. Let $U_{L_e} = U_{L_e}(X_1, X_2, \ldots, X_n)$ be a statistic calculated from the sample data satisfying $P(L_e \le U_{L_e}) = \gamma_2$, where the confidence level γ_2 does not depend on L_e. Then, U_{L_e} is an $100\gamma_2\%$ upper confidence bound for L_e. We note that

$$\begin{aligned} P(L_e \le U_{L_e}) &= P((n+\lambda)\hat{L}_e / L_e \ge (n+\lambda)\hat{L}_e / U_{L_e}) \\ &= P(\chi_n'^2(\lambda) \ge (n+\lambda)\hat{L}_e / U_{L_e}) = \gamma_2. \end{aligned} \tag{2.12}$$

Thus, $(n+\lambda)\hat{L}_e / U_{L_e} = \chi_n'^2(1-\gamma_2;\lambda)$, where $\chi_n'^2(1-\gamma_2;\lambda)$ is the $(1-\gamma_2)$th (lower) percentile of the $\chi_n'^2(\lambda)$ distribution. An $100\,\gamma_2\%$ upper confidence limit on L_e can be expressed, in terms of $\hat{L}_e$, as

$$U_{L_e} = \left[\frac{n+\lambda}{\chi_n'^2(1-\gamma_2;\lambda)}\right]\hat{L}_e. \tag{2.13}$$

The λ can be estimated by $\hat{\lambda} = n[(\bar{X} - T)/S_n]^2$ where $\bar{X} = \sum_{i=1}^n X_i / n$ and $S_n = [\sum_{i=1}^n (X_i - \bar{X})^2 / n]^{1/2}$. Substitute the results of L_Y and L_{Y_q} back to the equation, an $100\gamma\%$ lower confidence bound for Y_q and Y simultaneously can be expressed as:

$$\gamma = P\left(Y \ge 2\Phi(3C_L) - 1, Y_q \ge 2\Phi(3C_L) - 1 - \left[\frac{n+\hat{\lambda}}{\chi_n'^2(1-\gamma_2;\hat{\lambda})}\right]\hat{L}_e\right). \tag{2.14}$$

2.4 Application to Amplified Pressure Sensor (APS)

We consider the following case taken from a manufacturing factory making series of original equipment manufacturer (OEM) pressure sensors, which combines state-of-the-art pressure sensor technology with signal conditioning to produce a fully signal conditioned, amplified, temperature compensated sensor in a dual in-line package (DIP) configuration. Combining the sensor and the signal conditioning circuitry in a single package simplifies the use of advanced silicon micromachined pressure sensors. Now, the pressure sensor can be directly mounted to a standard printed circuit board and no additional components are required for obtaining an amplified high level, calibrated pressure measurement. The pressure sensors are based on highly stable, piezoresistive pressure sensor chips mounted on a ceramic substrate. Two different pin configurations of the APS part, one for classical thru-hole printed circuit board applications and one for surface mount applications are available. These are shown in Figures 4(a)-4(b). Note that the only difference between the two is the pins. The ceramic housing, cap and ports are identical between the two configurations.

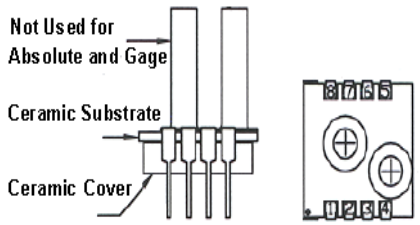

Figure 4(a). Standard Thru-Hole Pin Configuration for the APS.

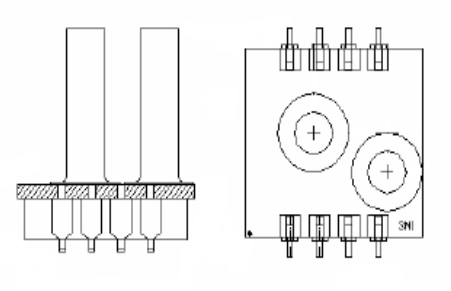

Figure 4(b). Surface-Mount Pin Configuration for the APS.

An electronically programmable application-specific integrated circuit (ASIC) is contained in the same package to provide calibration and temperature compensation. The model is designed for operating pressure ranges from 0-5 PSI up to 0-100 PSI. And the sensor output is ratio metric with the supply voltage. Some features of the model are: Wide selection of full-scale ranges to 100 PSI; low pressure (from 0-0.15 PSI FS) based on unique low-pressure die; amplified, calibrated, fully signal conditioned amplified output of 4.0 VDC FS span (0.5 to 4.5 V signal); output ratio metric with supply voltage; temperature compensation for span and offset; gage, differential, and absolute version; DIP package for convenient PC board mounting; small, lightweight package. Some typical applications are: barometric measurement; medical instrumentation; pneumatic control; gas flow; respirators and ventilators and ventilating and air-conditioning.

Amplified Pressure Product Capabilities

The series pressure product provides a significant advantage to the user due to a number of improvements associated with the technology used in fabricating this part. These advantages include integrated amplification, electronic-trim for more precise control of gain and offset, fewer external support components. The following notes are meant as an aid to the user to document some of these improvements. The amplified configuration has some key advantages but these also must be considered in designing the systems into which pressure sensor parts are used. For instance, a fairly standard "trick" when using an unamplified part in such absolute applications as barometric measurements is to use a 5 PSIA part. This allows it to operate in the 15 PSIA range with effectively 10 PSI overpressure, in order to get 3X more unamplified output from the part. The addition of amplification at the measurement site has several key advantages. One of those is the required support circuitry. The pressure sensor has been designed to eliminate the need for external components. The pressure sensor requires no external components. The pressure sensor model with the gain of the part testing is depicted as in Figure 5.

One of the key features of the pressure sensor is that it is electronically trimmed. As such, the part can be tested and verified before the final trim parameters are programmed. With the conventional laser-trimmed components, the final performance is set by how well the test system can measure millivolt

level signals and resistances ranging from less than 50 Ohms to over 5 MegOhm. All of this is done at the end of long test cables and this further makes measurements more uncertain. There are several alternative measures on the manufacturability of a part. Yield from a manufacturer's viewpoint is critical but so to is the distribution of parts as manufactured. The tighter the distribution on key parameters, the higher the quality of the part and the lower is the probability that the end-customer will get a part that will not meet the published specification.

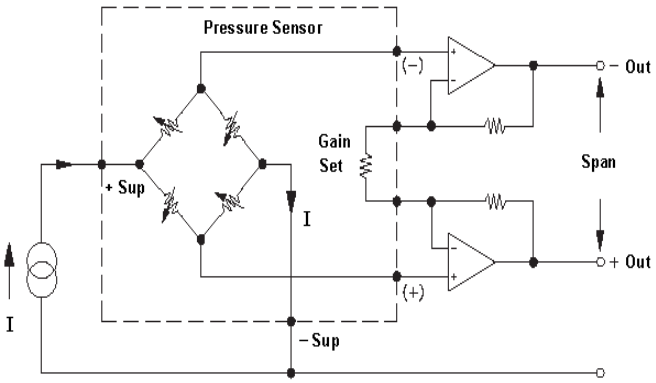

Figure 5. Application schematic with 1.5 mA drive at 25℃ after 10 second warm up.

Table 3. APS data of 100 measurements for the Zero and Span.

Zero (volt)				Span (volt)			
2.5445	2.5310	2.5204	2.5406	2.0512	2.0532	2.0396	2.0035
2.5455	2.5305	2.5418	2.5390	2.0594	2.0507	2.0382	2.0512
2.5338	2.5721	2.5430	2.5570	2.0517	2.0050	2.0276	1.9956
2.5482	2.5573	2.5403	2.5539	2.0038	2.0300	2.0719	2.0038
2.5306	2.5329	2.5391	2.5493	2.0532	2.0318	1.9957	2.0629
2.5471	2.5495	2.5202	2.5452	2.0235	2.0308	2.0226	2.0409
2.5482	2.5355	2.5470	2.5528	2.0373	1.9684	2.0113	2.0092
2.5474	2.5611	2.5434	2.5335	2.0501	2.0037	2.0295	2.0524
2.5532	2.5419	2.5327	2.5416	2.0575	2.0557	2.0333	2.0584
2.5511	2.5455	2.5618	2.5506	2.0070	2.0374	2.0563	2.0094
2.5490	2.5476	2.5490	2.5382	1.9716	2.0152	2.0392	2.0113
2.5543	2.5375	2.5454	2.5225	2.0390	2.0504	2.0529	2.0463
2.5454	2.5466	2.5253	2.5405	2.0316	1.9912	2.0824	2.0307
2.5279	2.5333	2.5586	2.5432	2.0000	2.0243	2.0825	2.0180
2.5381	2.5364	2.5563	2.5521	2.0102	1.9842	2.0300	2.0433
2.5453	2.5396	2.5493	2.5402	2.0112	2.0482	2.0440	1.9793
2.5379	2.5486	2.5382	2.5432	2.0024	2.0277	2.0199	2.0255
2.5270	2.5484	2.5461	2.5409	2.0638	2.0252	2.0006	2.0227
2.5367	2.5289	2.5335	2.5429	2.0518	2.0668	2.0142	2.0239
2.5518	2.5346	2.5265	2.5409	2.0105	2.0254	1.9966	2.0359
2.5462	2.5432	2.5390	2.5358	2.0536	2.0377	2.0162	1.9897
2.5542	2.5583	2.5361	2.5454	2.0275	2.0231	2.0636	2.0289
2.5398	2.5331	2.5440	2.5424	1.9993	1.9831	2.0533	2.0238
2.5203	2.5464	2.5270	2.5607	1.9985	2.0519	2.0041	2.0499
2.5291	2.5445	2.5360	2.5502	2.0254	2.0709	2.0162	2.0156

2.5 Q-Yield Calculation for Pressure Sensor Product

To illustrate how the proposed Q-yield lower confidence bound could be established and applied to actual data collected from the factories, we consider the following example taken from a company located on the Science-Based Industrial Park in Taiwan, which manufacturing and designing pressure sensor product. For a particular model of amplified pressure sensor process, capability analysis with focus on two key characteristics Span and Zero are taken. Span limits are $+/-100$ mV about a 2.000 volt target (USL = 2.100, LSL = 1.900, T = 2.000) and the Zero limits are set to $+/-80$ mV about a 2.500 volt target (USL = 2.580, LSL = 2.420, T = 2.500). Tight control of Zero and Span during test will make the part more capable. We test one hundred parts in each key characteristic, and the collected data are displayed in Table 3. Figures 6(a)-6(b) display the histogram with density of the 100 APS data measurements for the Zero and Span, respectively. Proceeding with the calculations with 95% level of confidence, we obtain the values of the calculated sample mean, sample derivation, estimated C_{pk} index values, the C_{pk} lower confidence bounds, estimated L_e values, the L_e upper confidence bounds, estimated yield, the yield lower confidence bounds, estimated Q-yield and the Q-yield lower confidence bounds as tabulated in Table 4.

Table 4. Calculated statistics, estimated process capability measures and corresponding lower confidence bound of the APS products.

	$\bar{X}$	S	$\hat{C}_{pk}$	C_L	$\hat{L}_e$	U_{L_e}	$\hat{Y}$	L_Y	$\hat{Y}_q$	L_{Y_q}
Zero	2.5424	0.0099	1.2705	1.0821	0.2959	0.3983	1.0000	0.9999	0.7041	0.6016
Span	2.0286	0.0246	0.9660	0.8165	0.1418	0.1908	1.0000	0.9962	0.8582	0.8054

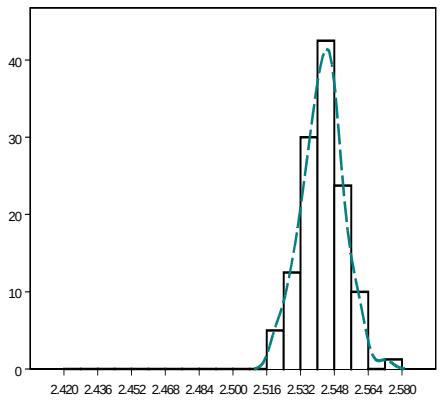

Figure 6(a). The histogram of the APS data measurements for the Zero.

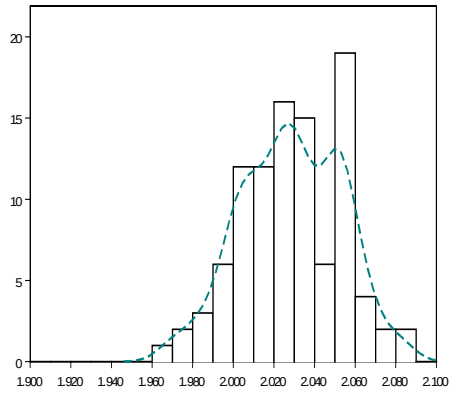

Figure 6(b). The histogram of the APS data measurements for the Span.

The plot of Q-yield versus yield is displayed in Figure 7. These two dimensions of product quality are useful because one dimension represents customer satisfaction while the other represents factory fulfillment. The triangle with vertices (0, 0), (1, 0) and (1, 1) contains the set of all (Y, Y_q). The objective of quality improvement is to move towards the point, (1, 1). The engineers can effectively monitor and get the most priority of all process characteristics simultaneously.

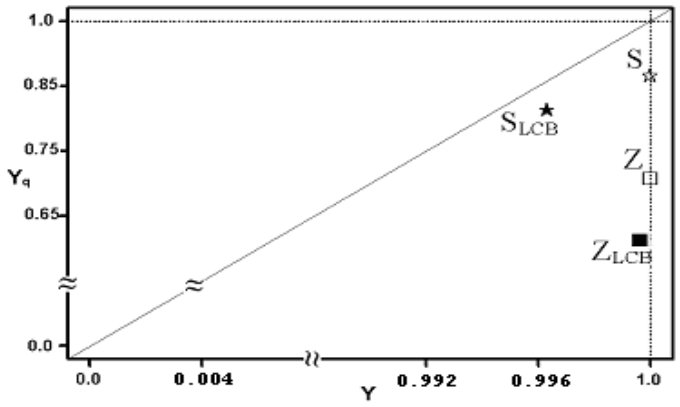

Figure 7. The plot of Q-yield versus yield.